Monthly Notices
of the
ROYAL ASTRONOMICAL SOCIETY

MNRAS **446,** 959–972 (2015) doi:10.1093/mnras/stu2100

Geometry of halo and Lissajous orbits in the circular restricted three-body problem with drag forces

Ashok Kumar Pal★ and Badam Singh Kushvah

Department of Applied Mathematics, Indian School of Mines, Dhanbad-826004, Jharkhand, India

Accepted 2014 October 8. Received 2014 October 2; in original form 2014 May 19

ABSTRACT

In this paper, we determine the effect of radiation pressure, Poynting–Robertson drag and solar wind drag on the Sun–(Earth–Moon) restricted three-body problem. Here, we take the larger body of the Sun as a larger primary, and the Earth+Moon as a smaller primary. With the help of the perturbation technique, we find the Lagrangian points, and see that the collinear points deviate from the axis joining the primaries, whereas the triangular points remain unchanged in their configuration. We also find that Lagrangian points move towards the Sun when radiation pressure increases. We have also analysed the stability of the triangular equilibrium points and have found that they are unstable because of the drag forces. Moreover, we have computed the halo orbits in the third-order approximation using the Lindstedt–Poincaré method and have found the effect of the drag forces. According to this prevalence, the Sun–(Earth–Moon) model is used to design the trajectory for spacecraft travelling under drag forces.

Key words: celestial mechanics – solar wind – planets and satellites: dynamical evolution and stability.

1 INTRODUCTION

During the last few years, many researchers have studied the effect of drag forces because of the significant role they have in the dynamical system. For example, Murray (1994) studied the dynamical effects of drag force in the circular restricted three-body problem and found the approximate location and stability properties of the Lagrangian points. Liou, Zook & Jackson (1995) examined the effects of radiation pressure, Poynting–Robertson (P–R) drag and solar wind drag on dust grains trapped in mean motion resonance with the Sun–Jupiter restricted three-body problem. Ishwar & Kushvah (2006) studied the linear stability of triangular equilibrium points in the generalized photogravitational restricted three-body problem with P–R drag and found that the triangular equilibrium points are unstable. Also, Kushvah (2008) determined the effect of radiation pressure on the equilibrium points in the generalized photogravitational restricted three-body problem, and noticed that the collinear points deviate from the axis joining the two primaries, whereas the triangular points are not symmetric because of the presence of radiation pressure. Moreover, Kumari & Kushvah (2013) studied the motion of the infinitesimal mass in the restricted four-body problem with solar wind drag and found the range of the radiation factor of the equilibrium points.

We know that the Lagrangian points are important for mission design and transfer of trajectories. A number of missions have been successfully operated in the vicinity of the Sun–Earth and Earth–Moon collinear Lagrangian points. In this regard, the *International Sun–Earth Explorer* (*ISEE*) programme was established as a joint project of the National Aeronautics and Space Administration (NASA) and the European Space Agency (ESA). *ISEE-3* was launched into a halo orbit around the Sun–Earth L_1 point in 1978, allowing it to collect data on solar wind conditions upstream from the Earth. Farquhar, Muhonen & Richardson (1977) had designed the *ISEE-3* scientific satellite in the vicinity of the Sun–Earth interior Lagrangian point to continuously monitor the space between the Sun and the Earth. *WIND* was launched on 1994 November 1 and was positioned in a sunward orbit. The *Solar and Heliospheric Observatory* (*SOHO*) project was launched in 1995 December to study the internal structure of the Sun. The *Advanced Composition Explorer* (*ACE*) was launched in 1997 and orbits the L_1 Lagrangian point, which is a point of the Sun–Earth gravitational equilibrium about 1.5 million km from the Earth and 148.5 million km from the Sun. *ARTHEMIS* was the first spacecraft to be in the vicinity of Earth–Moon Lagrangian point. In 2010 August, the *ARTHEMIS P1* spacecraft entered an orbit near the Earth–Moon L_2 point for approximately 131 d, before transferring to an L_1 quasi-halo orbit where it remained for an additional 85 d. On 2011 July 17, the *ARTHEMIS P2* spacecraft was successfully inserted into the Earth–Moon Lagrangian point orbit with an arrival near the L_2 point in 2010 October (Pavlak & Howell 2012). The *ARTHEMIS* Lagrangian point orbit design features quasi-halo orbits demonstrated recently by Folta et al. (2013).

To our knowledge, there have been numerous published papers that have extensively covered topics related to halo orbits, Lagrangian point satellite operations in general, and their

★ E-mail: ashokpalism@gmail.com

applications within the Earth–Moon and Sun–Earth system. For more information on halo orbits, we refer to the three-dimensional periodic halo orbits near the collinear Lagrangian points in the restricted three-body problem obtained by Howell (1984). She obtained orbits that increase in size when increasing the mass parameter μ. Clarke (2003, 2005) discussed a discovery mission concept that utilizes occultations from a lunar halo orbit by the Moon to enable detection of terrestrial planets. Breakwell & Brown (1979) has computed halo orbits around the Earth–Moon L_2 point. Calleja et al. (2012) computed the unstable manifolds of selected vertical and halo orbits, which in several cases have led to the detection of heteroclinic connections from such a periodic orbit to invariant tori. Other authors have carried out similar work (Di Giamberardino & Monaco 1992; Farquhar 2001; Kim & Hall 2001; Junge et al. 2002; Kolemen, Kasdin & Gurfil 2007; Hill & Born 2008). However, they ignored the drag force, although Eapen & Sharma (2014) have studied the halo orbits at the Sun–Mars L_1 Lagrangian point in the photogravitational restricted three-body problem and have found that as the radiation pressure increases, the transition from the Mars-centric path to the heliocentric path is delayed.

In this paper, we study the effect of radiation pressure, P–R drag, and solar wind drag on the Lagrangian points and use the Lindstedt–Poincaré method to compute halo orbits in vicinity of the L_1 point of the Sun–Earth–Moon system. This paper is organized as follows. In Section 2, we recall some well-known facts about the circular restricted three-body problem with drag forces (i.e. its equations of motion, equilibrium points and stability). In Section 3, we describe the motion near the Lagrangian point L_1, and use the Lindstedt–Poincaré method to compute the halo orbits. In Section 4, we discuss our results. Finally, in Appendix A, we provide all the coefficients.

2 MATHEMATICAL FORMULATION OF THE PROBLEM AND EQUATIONS OF MOTION

We formulate the Sun–Earth–Moon system with the radiation pressure, P–R drag and solar wind drag (Parker 1965) and proceed with the problem as follows (Liou et al. 1995). The equations of motion in the rotating reference frame are

$$\ddot{x} - 2\dot{y} = \frac{\partial U}{\partial x} + (1+sw)F_x, \tag{1}$$

$$\ddot{y} + 2\dot{x} = \frac{\partial U}{\partial y} + (1+sw)F_y, \tag{2}$$

$$\ddot{z} = \frac{\partial U}{\partial z} + (1+sw)F_z, \tag{3}$$

where

$$U = \frac{(1-\beta)(1-\mu)}{r_1} + \frac{\mu}{r_2} + \frac{1}{2}(x^2+y^2), \tag{4}$$

and the drag force components are

$$F_x = \frac{-\beta(1-\mu)}{cr_1^2}\left\{\frac{[(x+\mu)\dot{x}+(\dot{y}-\mu)y+z\dot{z}](x+\mu)}{r_1^2} + (\dot{x}-y)\right\}, \tag{5}$$

$$F_y = \frac{-\beta(1-\mu)}{cr_1^2}\left\{\frac{[(x+\mu)\dot{x}+(\dot{y}-\mu)y+z\dot{z}]y}{r_1^2} + (\dot{y}+x)\right\}, \tag{6}$$

$$F_z = \frac{-\beta(1-\mu)}{cr_1^2}\left\{\frac{[(x+\mu)\dot{x}+(\dot{y}-\mu)y+z\dot{z}]z}{r_1^2} + \dot{z}\right\}. \tag{7}$$

It is supposed that m_1 is the mass of the Sun and m_2 is the mass of the Earth plus Moon, and hence the mass parameter $\mu = m_2/(m_1+m_2)$. However, the definition of the mass parameter μ is different from that of Liou et al. (1995). They have used μ_1 and μ_2 to represent the masses of the Sun and Jupiter, respectively, whereas in the present problem the masses are represented by m_1 and m_2. Here, β is the ratio of the radiation pressure force to the solar gravitation force, sw is the ratio of solar wind drag to P–R drag (Burns, Lamy & Soter 1979; Gustafson 1994) and c is the unitless speed of light. The unit of mass is taken in such a way that $G(m_1+m_2)=1$; the unit of distance is taken as the distance of the centre of mass (of the Earth–Moon) to the Sun, whereas the unit of time is taken to be the time period of the rotating frame.

In order to calculate the Lagrangian equilibrium points, we solve equations (1)–(3) with the condition that all derivatives are zero, and we obtain

$$x - \frac{(1-\beta)(1-\mu)}{r_1^3}(x+\mu) - \frac{\mu}{r_2^3}(x+\mu-1) + \frac{(1+sw)\beta(1-\mu)}{r_1^2}\left[\frac{\mu y(x+\mu)}{cr_1^2} + \frac{y}{c}\right] = 0, \tag{8}$$

$$y\left[1 - \frac{(1-\beta)(1-\mu)}{r_1^3} - \frac{\mu}{r_2^3}\right] + \frac{(1+sw)\beta(1-\mu)}{r_1^2} \times \left[\frac{\mu y^2}{cr_1^2} - \frac{x}{c}\right] = 0, \tag{9}$$

$$z\left[\frac{(1-\beta)(1-\mu)}{r_1^3} + \frac{\mu}{r_2^3} - \frac{(1+sw)\beta(1-\mu)\mu y}{cr_1^4}\right] = 0. \tag{10}$$

From equation (10), we obtain two possible solutions, either $z=0$ or $z\neq 0$. If $z\neq 0$, then

$$\frac{(1-\beta)(1-\mu)}{r_1^3} + \frac{\mu}{r_2^3} = \frac{(1+sw)\beta(1-\mu)\mu y}{cr_1^4}. \tag{11}$$

From equation (11), with $\beta = 0$ (i.e. no radiation pressure is taken into account), we obtain

$$\frac{1-\mu}{r_1^3} = -\frac{\mu}{r_2^3}. \tag{12}$$

From the right-hand side of equation (12), because $\mu > 0$, and also r_2 is the distance of the infinitesimal body from the second primary, we find that

$$\frac{1-\mu}{r_1^3} = -\frac{\mu}{r_2^3} < 0. \tag{13}$$

This gives $\mu > 1$, which is never possible. Therefore, at $\beta = 0$, there are no equilibrium points outside the xy-plane.

Again, with $z \neq 0$ and if $0 < \beta < 1$, then it is obvious from equation (11) that the only possible solution is to have $y > 0$. From equations (9) and (11), we obtain

$$y - \frac{(1+sw)\beta(1-\mu)x}{cr_1^2} = 0. \tag{14}$$

With the condition that $y > 0$, equation (14) gives one possible solution $x > 0$, and therefore $x+\mu > 0$. Now, we divide both sides of equation (8) by $(x+\mu)$, and using equation (11), we obtain

$$\frac{x}{x+\mu} + \frac{\mu}{r_2^3(x+\mu)} + \frac{(1+sw)\beta(1-\mu)y}{cr_1^2(x+\mu)} = 0. \tag{15}$$

For $x > 0$ and $y > 0$, the left-hand side of equation (15) has a non-zero quantity. Therefore, z must be zero and have no equilibrium points outside the xy-plane.

Simmons, McDonald & Brown (1985) have shown that out-of-plane equilibrium points occur if $(1 - \beta_1)/(1 - \beta_2) < 0$, where $\beta_{1,2}$ are the ratios of the magnitudes of radiation to the gravitational forces from $m_{1,2}$. However, in the present Sun–Earth–Moon system, only the Sun is a radiating body. Therefore, $\beta_2 = 0$ and $\beta_1 = \beta > 1$, which is not possible. Consequently, out-of-plane equilibrium points do not exist in the present model.

Thus, for $z = 0$, we solve equations (8) and (9) using Taylor series expansions in r_1 and r_2 and some approximations, as in Murray & Dermott (1999). The general solutions are given by

$$x^* = x_0 + \Delta x, \quad \text{and} \quad y^* = y_0 + \Delta y. \tag{16}$$

Here, Δx and Δy are the small quantities that are introduced for drag forces and (x_0, y_0) is a solution of the equations when there is no drag force. The corresponding distances of the infinitesimal body to the masses m_1 and m_2 are given by

$$r_1^* = \sqrt{(x^* + \mu)^2 + y^{*2} + z^{*2}} \tag{17}$$

and

$$r_2^* = \sqrt{(x^* + \mu - 1)^2 + y^{*2} + z^{*2}}. \tag{18}$$

We use the Taylor series expansions around (x_0, y_0) and neglect second- and higher-order terms in Δx and Δy. Then, we solve the simultaneous equations in Δx and Δy ($\because z_0 = 0$ for all Lagrangian points). We obtain following expressions of Δx and Δy for all the Lagrangian points with a fixed value of $sw = 0.35$ (Gustafson 1994):

for L_1,

$$\Delta x = 0.494997 - \frac{2.19061}{4.42551 - \beta},$$

$$\Delta y = \frac{0.470726(-3.74923 \times 10^{-9} + 4.23594 \times 10^{-10}\beta)}{(-4.42551 + \beta)(-2.97008 + \beta)};$$

for L_2,

$$\Delta x = \frac{0.505037(-1.23265 \times 10^{-15} + \beta)}{-4.57611 + \beta},$$

$$\Delta y = \frac{0.530994(-3.57762 \times 10^{-9} + 3.90903 \times 10^{-10}\beta)\beta}{(-4.57611 + \beta)(-3.03032 + \beta)};$$

for L_3,

$$\Delta x = \frac{0.5\beta}{1.5 - \beta},$$

$$\Delta y = \frac{0.500004(1.22068 \times 10^{-9} - 4.06893 \times 10^{-10})\beta}{(-1.5 + \beta)(3.34357 \times 10^{-6} + \beta)};$$

for $L_{4,5}$,

$$\Delta x = \frac{0.25\beta(0.0000126643 + \beta)(3.00001 + \beta)}{(-1.5 + \beta)(5.83558 \times 10^{-6} + \beta)(3.00001 + \beta)}, \tag{19}$$

$$\Delta y = \pm\frac{0.500002(3.08248 \times 10^{-6} + 0.866021\beta)\beta}{(-1.5 + \beta)(5.83558 \times 10^{-6} + \beta)}. \tag{20}$$

The effect of β in Δx on the L_1 and L_2 points is shown in the top panel of Fig. 1, whereas the bottom panel is for the L_3 point. For the L_1 and L_2 points, the effect of β is approximately equal

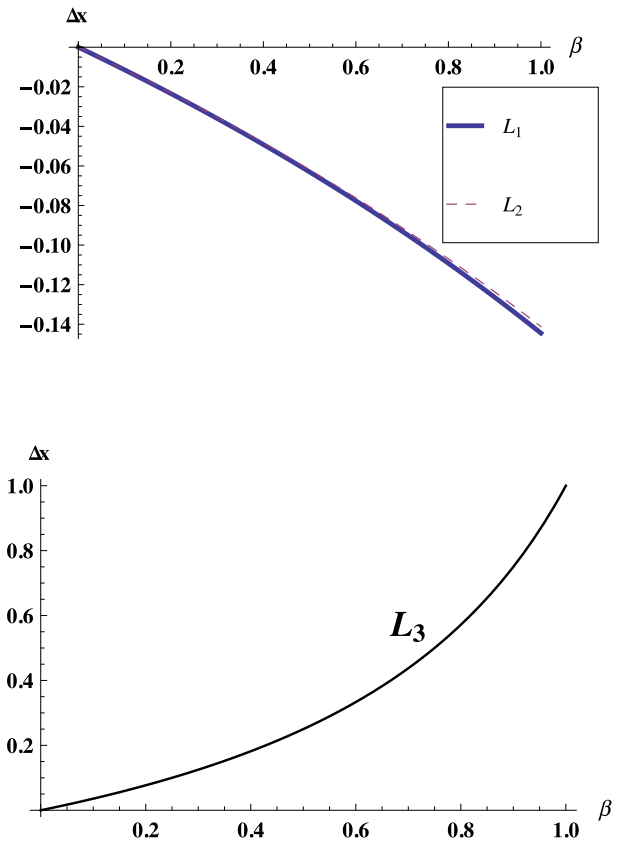

Figure 1. Effect of β on the x coordinate in the $L_{1,2,3}$ points.

and Δx is increasing negatively (i.e. both the L_1 and L_2 points tend towards the Sun with increasing radiation pressure). For the L_3 point, Δx increases positively when β increases, and therefore the Lagrangian point L_3 also tends towards the Sun. Δy corresponds to the case when $L_{1,2,3}$ increase negatively, for an increasing value of β, which is shown in Fig. 2. Therefore, when the radiation pressure increases, the collinear points perturb from their collinearity and tend towards the radiating body of the Sun.

The different Lagrangian points L_i, $(i = 1, 2, 3)$ at different values of β are presented in Table 1. The effect of radiation pressure in Δx of $L_{4,5}$ is the same, as shown in Fig. 3, while Fig. 4 shows that there is a symmetrical change in Δy of L_4 and L_5. These equilibrium points also tend towards the Sun symmetrically when β increases. The different triangular points $L_{4,5}$ at different values of β are shown in Table 2.

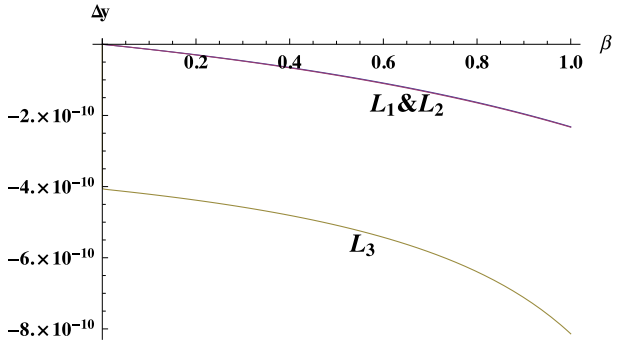

Figure 2. Effect of β on the y coordinate in the $L_{1,2,3}$ points.

Table 1. Lagrangian equilibrium points L_i, $(i = 1, 2, 3)$ with $sw = 0.35$.

β	L_1	L_2	L_3
0.0	(0.989991, 0)	(1.01007, 0)	(− 1.00000326495, 0)
0.1	(0.978547, -1.40554×10^{-11})	(0.998787, -1.43251×10^{-11})	(− 0.964289, -4.21415×10^{-10})
0.2	(0.966562, -2.94742×10^{-11})	(0.986989, -3.0005×10^{-11})	(− 0.92308, -4.3819×10^{-10})
0.3	(0.953996, -4.64359×10^{-11})	(0.974638, -4.72137×10^{-11})	(− 0.875003, -4.57754×10^{-10})
0.4	(0.940805, -6.51505×10^{-11})	(0.961696, -6.6153×10^{-11})	(− 0.818185, -4.80874×10^{-10})
0.5	(0.926942, -8.58655×10^{-11})	(0.948119, -8.70629×10^{-11})	(− 0.750004, -5.08618×10^{-10})
0.6	(0.912355, -1.08874×10^{-10})	(0.93386, -1.10221×10^{-10})	(− 0.666671, -5.42526×10^{-10})
0.7	(0.896984, -1.34524×10^{-10})	(0.918864, -1.35961×10^{-10})	(− 0.562504, -5.84912×10^{-10})
0.8	(0.880766, -1.63235×10^{-10})	(0.903074, -1.64679×10^{-10})	(− 0.428576, -6.39407×10^{-10})
0.9	(0.863627, -1.95512×10^{-10})	(0.886425, -1.96851×10^{-10})	(− 0.250006, -7.12067×10^{-10})
1.0	(0.845488, -2.31971×10^{-10})	(0.868845, -2.33054×10^{-10})	(-7.51792×10^{-6}, -8.13791×10^{-10})

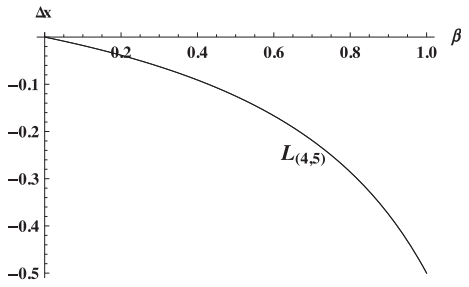

Figure 3. Effect of β on the x coordinate of triangular points.

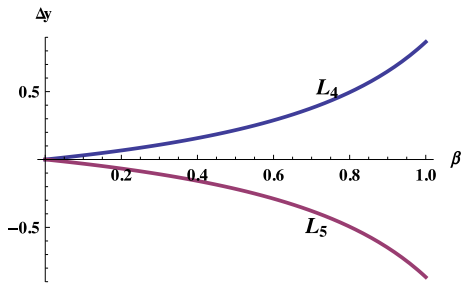

Figure 4. Effect of β on the y coordinate of triangular points.

Table 2. Triangular equilibrium points with $sw = 0.35$.

β	$L_{(4,5)}$
0.0	(0.499997, ±0.866025)
0.1	(0.482139, ±0.835096)
0.2	(0.461534, ±0.799408)
0.3	(0.437496, ±0.757773)
0.4	(0.409086, ±0.708567)
0.5	(0.374995, ±0.64952)
0.6	(0.333329, ±0.577351)
0.7	(0.281245, ±0.487141)
0.8	(0.214281, ±0.371155)
0.9	(0.124995, ±0.216509)
1.0	(-5.81166×10^{-6}, ±3.08134 × 10^{-6})

2.1 Stability of the equilibrium points

The locations of equilibrium points do not affect our knowledge of their stability. We now consider the stability property by using the standard technique of linearizing the perturbation equations in the vicinity of an equilibrium point. Our approach is based on that of Schuerman (1980) and Murray (1994).

Consider a small displacement from the equilibrium position (x^*, y^*), and let the solution for the subsequent motion be of the form $x = x^* + X$, $y = y^* + Y$, where

$$X = X_0 e^{\lambda t}, \qquad Y = Y_0 e^{\lambda t}, \tag{21}$$

and X_0, Y_0 and λ, are constants. Using these substitutions in equations (8) and (9), and using Taylor series expansion, the following simultaneous linear equations in X and Y are given as

$$X\left\{\lambda^2 + \frac{(1-\beta)(1-\mu)}{r_1^{*3}}\left[1 - \frac{3(x^*+\mu)^2}{r_1^{*2}}\right] + \frac{\mu}{r_2^{*3}} \times \left[1 - \frac{3(x^*+\mu-1)^2}{r_2^{*3}}\right] - 1 - (1+sw)\left[\left(\lambda\frac{\partial F_x}{\partial \dot{x}}\right)_* + \left(\frac{\partial F_x}{\partial x}\right)_*\right]\right\} + Y\left\{-2\lambda - \frac{3(1-\beta)(1-\mu)y^*(x^*+\mu)}{r_1^{*5}} - \frac{3\mu y^*(x^*+\mu-1)}{r_2^{*5}} - (1+sw)\left[\left(\lambda\frac{\partial F_x}{\partial \dot{y}}\right)_* + \left(\frac{\partial F_y}{\partial y}\right)_*\right]\right\} = 0 \tag{22}$$

and

$$X\left\{2\lambda - \frac{3(1-\beta)(1-\mu)y^*(x^*+\mu)}{r_1^{*5}} - \frac{3\mu y^*(x+\mu-1)}{r_2^{*5}} - (1+sw)\left[\left(\lambda\frac{\partial F_y}{\partial \dot{x}}\right)_* - \left(\frac{\partial F_y}{\partial x}\right)\right]\right\} + Y\left\{\lambda^2 + \frac{(1-\mu)(1-\beta)}{r_1^{*3}}\left(1 - \frac{3y^{*2}}{r_1^{*2}}\right) + \frac{\mu}{r_2^{*3}}\left(1 - \frac{3y^{*2}}{r_2^{*2}}\right) - 1 - (1+sw)\left[\lambda\left(\frac{\partial F_y}{\partial \dot{y}}\right)_* - \left(\frac{\partial F_y}{\partial y}\right)_*\right]\right\} = 0, \tag{23}$$

where $(\,)_*$ denotes the evaluation of a partial derivative at the displaced equilibrium point. We can now rewrite equations (22) and (23) as

$$X[\lambda^2 + a^* - d^* - 1 - (1+sw)(\lambda K_{x,\dot{x}} + K_{x,x})] + Y[-2\lambda - c^* - (1+sw)(\lambda K_{x,\dot{y}} + K_{x,y})] = 0, \tag{24}$$

$$X[2\lambda - c^* - (1+sw)(\lambda K_{y,\dot{x}} + K_{y,x})] + Y[\lambda^2 + a^* - b^* - 1 - (1+sw)(\lambda K_{y,\dot{y}} + K_{y,y})] = 0, \tag{25}$$

where the constants are

$$a^* = \frac{(1-\beta)(1-\mu)}{r_1^{*3}} + \frac{\mu}{r_2^{*3}}, \tag{26}$$

$$b^* = 3\left[\frac{(1-\beta)(1-\mu)}{r_1^{*5}} + \frac{\mu}{r_2^{*5}}\right] y^{*2}, \tag{27}$$

$$c^* = 3\left[\frac{(1-\beta)(1-\mu)(x^*+\mu)}{r_1^{*5}}. + \frac{\mu(x^*+\mu-1)}{r_2^{*5}}\right] y^*, \tag{28}$$

$$d^* = 3\left[\frac{(1-\beta)(1-\mu)(x^*+\mu)^2}{r_1^{*5}} + \frac{\mu(x^*+\mu-1)^2}{r_2^{*5}}\right], \tag{29}$$

and

$$K_{x,x} = \left(\frac{\partial F_x}{\partial x}\right)_*, \qquad K_{x,\dot{x}} = \left(\frac{\partial F_x}{\partial \dot{x}}\right)_*, \tag{30}$$

$$K_{x,y} = \left(\frac{\partial F_x}{\partial y}\right)_*, \qquad K_{x,\dot{y}} = \left(\frac{\partial F_x}{\partial \dot{y}}\right)_*, \tag{31}$$

$$K_{y,x} = \left(\frac{\partial F_y}{\partial x}\right)_*, \qquad K_{y,\dot{x}} = \left(\frac{\partial F_y}{\partial \dot{x}}\right)_*, \tag{32}$$

$$K_{y,y} = \left(\frac{\partial F_y}{\partial y}\right)_*, \qquad K_{y,\dot{y}} = \left(\frac{\partial F_y}{\partial \dot{y}}\right)_*. \tag{33}$$

The condition for the determinant of the linear equations defined by equations (24) and (25) needs to be zero. Neglecting the terms of $O(K^2)$, we obtain the characteristic equation as

$$\lambda^4 + a_3\lambda^3 + (a_{20}+a_2)\lambda^2 + a_1\lambda + (a_{00}+a_0) = 0, \tag{34}$$

where the approximate expressions for constants a_{00} and a_{20}, and the drag force terms $a_i (i = 0, 1, 2, 3)$ are given in Appendix A.

If we take $K = 0$, then the characteristic equation reduces to the following form

$$\lambda^4 + a_{20}\lambda^2 + a_{00} = 0, \tag{35}$$

which gives the classical solutions. The four roots in the classical problem occur as real and pure imaginary pairs, as in the case of each L_i, $(i = 1, 2, 3)$, whereas two pure imaginary pairs occur in the case of L_4 and L_5. The stability of the given equilibrium point depends on the sign and value of the roots of the characteristic equation. If any of the roots has a positive real part, the motion is unstable to small displacements with exponential growth, whereas in the classical case, the L_4 and L_5 points are linearly stable to small displacements in the system.

If we restrict our analysis to L_4 and L_5, the four roots of the characteristic equation, without drag forces, are given as

$$\lambda_n = \pm Zi, \quad (n = 1, 2, 3, 4), \tag{36}$$

where

$$Z = \sqrt{\frac{a_{20} \pm \sqrt{a_{20}^2 - 4a_{00}}}{2}}. \tag{37}$$

In the presence of drag forces, we assume that the roots are in the following form

$$\lambda = \eta Z \pm i(1+\gamma)Z, \tag{38}$$

that is,

$$\lambda_{1,2} = \eta Z + (1+\gamma)Zi, \tag{39}$$

$$\lambda_{3,4} = \eta Z - (1+\gamma)Zi, \tag{40}$$

where γ and η are small real quantities. With the help of equations (34), (39) and (40), neglecting the product of γ and then η with a_i, and solving the real and imaginary parts, we obtain

$$\eta = \frac{(a_3 Z^2 - a_1)}{2Z(-2Z^2 + a_{20})} \tag{41}$$

and

$$\gamma = \frac{(a_{00}+a_0) - (a_{20}+a_2)Z^2 + Z^4}{2Z^2(a_{20} - 2Z^2)}. \tag{42}$$

In all the cases, the real part of at least one characteristic root is positive. Therefore, the equilibrium point is a saddle point.

3 COMPUTATION OF HALO ORBIT

In order to discuss the motion near the Lagrangian point of the system, we choose a coordinate system centred at the Lagrangian point L_1 in the rotating reference frame. The equations of motion of an infinitesimal body are obtained by translating the origin to the location of L_1. The referred translation is given as

$$x = X - 1 + \mu + \gamma, \qquad y = Y - l \qquad \text{and} \qquad z = Z. \tag{43}$$

In this new coordinate system, the variables x, y and z are scaled. The distances between L_1 and the smaller primary are γ in the x-axis and l in the y-axis. Using these facts in equations (1)–(3), we obtain the equations of motion with the help of Legendre polynomials for expanding the non-linear terms and considering the linear parts, and we can write

$$\ddot{x} - 2\dot{y} - x\nu_{10} + y\nu_{11} = 0, \tag{44}$$

$$\ddot{y} + 2\dot{x} - y\nu_{21} - x\nu_{20} = 0, \tag{45}$$

$$\ddot{z} + \nu_* z = 0. \tag{46}$$

All the coefficients are given in Appendix A. Here, the z-axis solution is simple harmonic, because $\nu_* > 0$. However, the motion in the xy-plane is coupled. Solving equations (44) and (45), the characteristic equation has two real and two complex roots. The complex roots are not pure imaginary but the real parts of the complex roots are very small with respect to the age of the Solar system. Therefore, we neglect them and the roots are $\pm\alpha$ and $\pm i\lambda$, where

$$\alpha = \pm\sqrt{\frac{-4 + \nu_{21} + \nu_{10} + \sqrt{(4 - \nu_{21} - \nu_{10})^2 - 4\zeta_1}}{2}} \tag{47}$$

and

$$\lambda = \pm\sqrt{\frac{4 - (\nu_{21} + \nu_{10}) + \sqrt{(4 - \nu_{21} - \nu_{10})^2 - 4\zeta_1}}{2}}. \tag{48}$$

All the coefficients are given in Appendix A. Because the two real roots are opposite in sign, arbitrarily chosen initial conditions give rise to unbounded solutions as time increases. If, however, the initial conditions are restricted and only a non-divergent mode is allowed, the xy-solution will be bounded. In this case, the linearized equations have solutions of the form

$$x(t) = -A_x \cos(\lambda t + \phi), \tag{49}$$

$$y(t) = \kappa A_x[2\lambda \sin(\lambda t + \phi) - \nu_{11} \cos(\lambda t + \phi)], \tag{50}$$

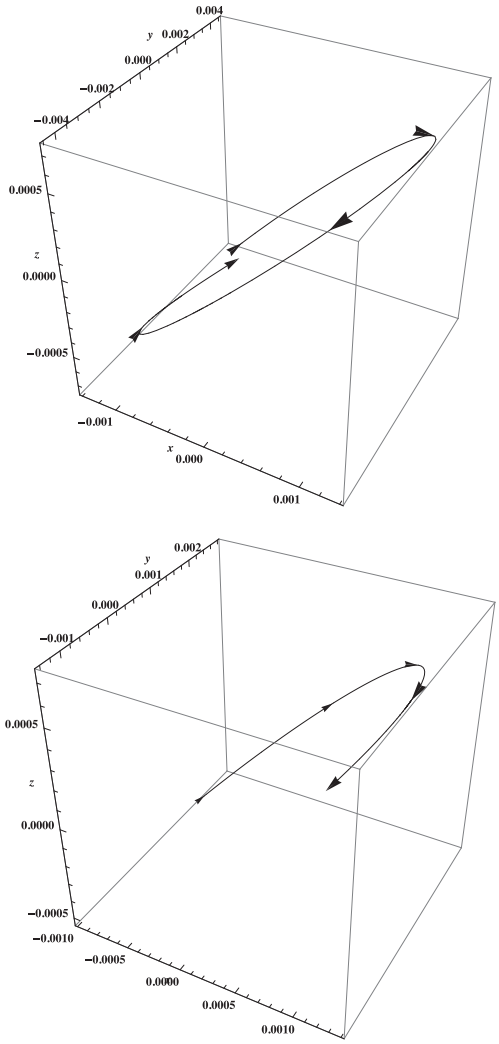

Figure 5. Effect of β in one period.

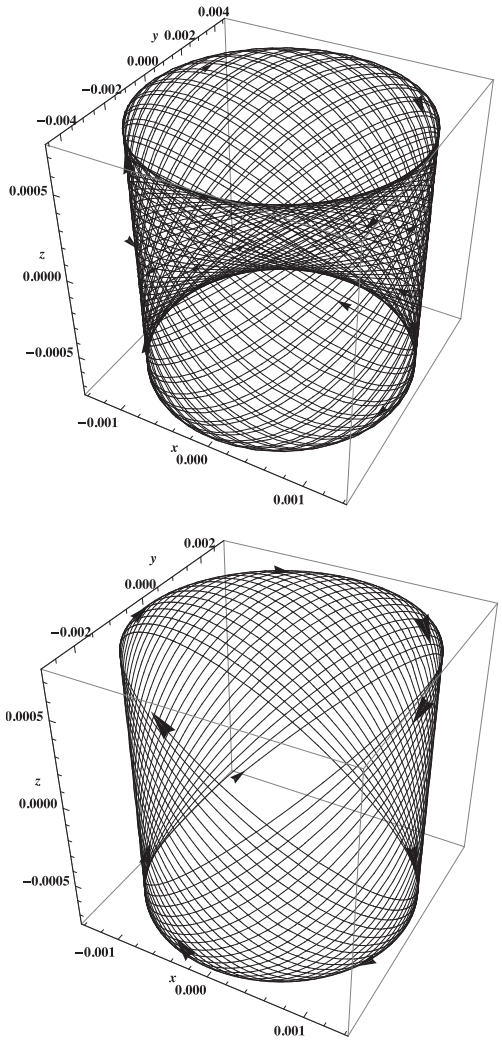

Figure 6. Effect of β on the Lissajous orbits: upper panel, $\beta = 0$; lower panel, $\beta = 0.2$.

$$z(t) = A_z \sin(\sqrt{\nu_*}t + \psi), \tag{51}$$

with

$$\kappa = \frac{\lambda^2 + \nu_{10}}{4\lambda^2 + \nu_{11}^2}. \tag{52}$$

The in-plane and out-of-plane frequencies are not equal, they are incommensurable. Then, the linearized motion produces the Lissajous-type trajectories for the Sun–(Earth–Moon) system around L_1. When the radiation pressure increases, the phase difference of the trajectories decreases. When there is no drag force (i.e. $\beta = 0$), the trajectory of the Lissajous orbit completes one period approximately at $t = 3.0$, but when the radiation pressure force increases (i.e. $\beta = 0.2$), it does not complete its period at that time, as shown in Fig. 5. Therefore, the period increases with an increase in the value of β. Also, because of the increasing value of β, the trajectories shrink in its amplitude.

Fig. 6 shows the Lissajous orbits with $\beta = 0$ and $\beta = 0.2$ shown in the upper and lower panels, respectively. Figs 7, 8 and 9 show the projections in the xy-, xz- and yz-plane, respectively, with the different values of β. Here, black, blue and red coloured orbits are shown with $\beta = 0$, 0.05 and 0.1, respectively. Clearly, the orbits shrink when β increases.

3.1 Periodic orbits using the Lindstedt–Poincaré method

The equations of motions can be written using the Legendre polynomials P_n. A third-order approximation was used in the circular restricted three-body problem without any drag force by Richardson (1980). Here, we include P–R drag and solar wind drag, and then find the third-order approximation as described by Thurman & Worfolk (1996):

$$\begin{aligned}\ddot{x} - 2\dot{y} &= x\nu_{10} - y\nu_{11} + x^2\nu_{12} + y^2\nu_{13} + z^2\nu_{14} \\ &\quad - xy\nu_{15} + x^3\nu_{16} + y^3\nu_{17} + xy^2\nu_{18} + xz^2\nu_{19} \\ &\quad + x^2y\nu_{190} + yz^2\nu_{191} + \nu^* + O(4),\end{aligned} \tag{53}$$

$$\begin{aligned}\ddot{y} + 2\dot{x} &= x\nu_{20} + y\nu_{21} + x^2\nu_{22} + y^2\nu_{23} + z^2\nu_{24} \\ &\quad + xy\nu_{25} + x^3\nu_{26} + y^3\nu_{27} + xy^2\nu_{29} + xz^2\nu_{290} \\ &\quad + x^2y\nu_{291} + yz^2\nu_{292} + \nu_{**} + O(4),\end{aligned} \tag{54}$$

$$\begin{aligned}\ddot{z} + \nu_* z &= xz\nu_{30} + yz\nu_{31} + x^2z\nu_{32} + xyz\nu_{33} \\ &\quad + y^2z\nu_{34} + z^3\nu_{35} + O(4).\end{aligned} \tag{55}$$

All the coefficients are given in Appendix A.

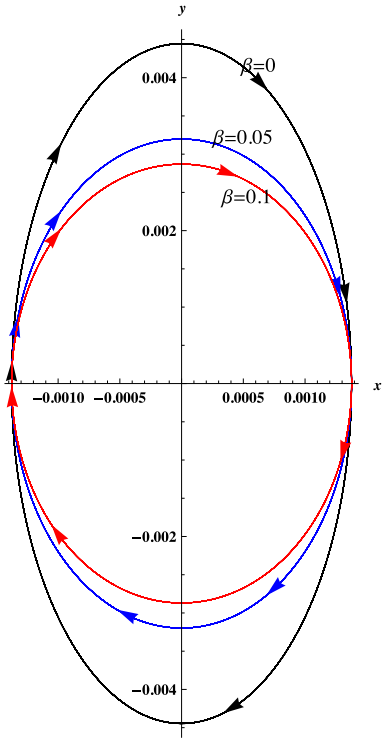

Figure 7. Projection on the xy −plane.

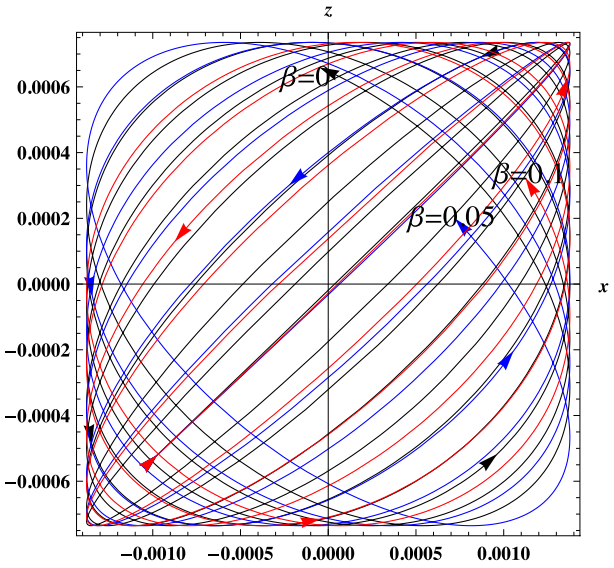

Figure 8. Projection on the xz −plane.

3.2 Correction term

For the construction of higher-order applications, we linearize equation (55) and introduce a correction term

$$\Delta = \lambda^2 - \nu_*, \tag{56}$$

on the right-hand side. The new third-order z equation becomes

$$\ddot{z} + \lambda^2 z = xz\nu_{30} + yz\nu_{31} + x^2 z\nu_{32} + xyz\nu_{33} + y^2 z\nu_{34} + z^3\nu_{35} + \Delta z + O(4). \tag{57}$$

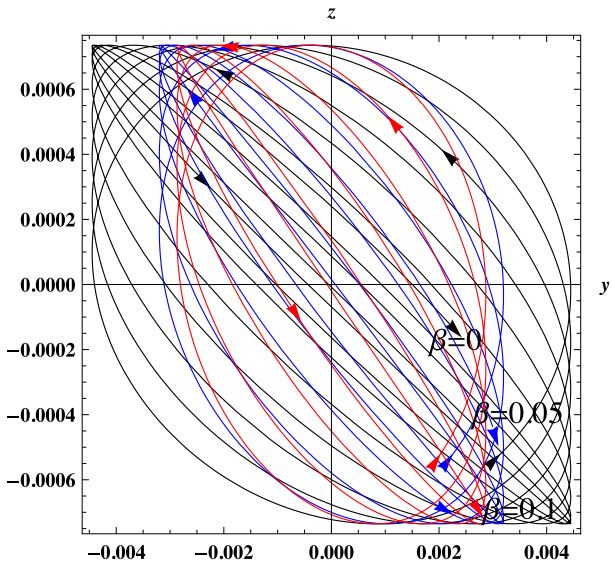

Figure 9. Projection on the yz −plane.

Richardson (1980) developed a third-order periodic solution using the Lindstedt–Poincaré type of successive approximations. We follow their work with the P–R drag and solar wind drag, by removing secular terms. A new independent variable τ and a frequency connection ω are introduced via $\tau = \omega t$. Then, the equations of motion at the second degree including the P–R drag and solar wind drag are given as

$$\omega^2 x'' - 2\omega y' = x\nu_{10} - y\nu_{11} + x^2\nu_{12} + y^2\nu_{13} + z^2\nu_{14} - xy\nu_{15} + x^3\nu_{16} + y^3\nu_{17} + xy^2\nu_{18} + xz^2\nu_{19} + x^2 y\nu_{190} + yz^2\nu_{191} + \nu^* + O(4), \tag{58}$$

$$\omega^2 y'' + 2\omega x' = x\nu_{20} + y\nu_{21} + x^2\nu_{22} + y^2\nu_{23} + z^2\nu_{24} + xy\nu_{25} + x^3\nu_{26} + y^3\nu_{27} + xy^2\nu_{29} + xz^2\nu_{290} + x^2 y\nu_{291} + yz^2\nu_{292} + \nu_{**} + O(4), \tag{59}$$

$$\omega^2 z'' + \lambda^2 z = xz\nu_{30} + yz\nu_{31} + xy\nu_{32} + x^2\nu_{33} + x^2 z\nu_{32} + xyz\nu_{33} + y^2 z\nu_{34} + z^3\nu_{35} + \Delta z + O(4), \tag{60}$$

where a prime denotes d/dτ. Because of perturbation analysis, we assume solutions in the following forms:

$$x(\tau) = \epsilon x_1(\tau) + \epsilon^2 x_2 + \epsilon^3 x_3 \ldots; \tag{61}$$

$$y(\tau) = \epsilon y_1(\tau) + \epsilon^2 y_2 + \epsilon^3 y_3 \ldots; \tag{62}$$

$$z(\tau) = \epsilon z_1(\tau) + \epsilon^2 z_2 + \epsilon^3 z_3 \ldots; \tag{63}$$

$$\omega = 1 + \epsilon\omega_1(\tau) + \epsilon^2\omega_2 + \epsilon^3\omega_3 \ldots.. \tag{64}$$

We substitute these into the equations of motion and equate components of the same order of ϵ. We find the first-, second- and third-order equations and their solutions.

3.3 First-order equations

To find the first-order approximation, we use equations (58)–(64) and compare the coefficients of the first-order terms in ϵ on both sides. We obtain the following equations:

$$x'' - 2y' = x\nu_{10} - y\nu_{11} + x^2\nu_{12}; \tag{65}$$

$$y'' + 2x' = x\nu_{20} + y\nu_{21}; \tag{66}$$

$$z'' + \lambda^2 z = 0. \tag{67}$$

From the above equations, we find the following bounded solutions:

$$x_1(\tau) = -A_x \cos(\lambda\tau + \phi); \tag{68}$$

$$y_1(\tau) = \kappa A_x[2\lambda \sin(\lambda\tau + \phi) - \nu_{10}\cos(\lambda\tau + \phi)]; \tag{69}$$

$$z_1(\tau) = A_z \sin(\lambda\tau + \psi). \tag{70}$$

In order to avoid secular solutions, we need constraints on the constants A_x, A_z, ϕ and ψ, but for now they are arbitrary.

3.4 Second-order equations

The order of the $O(\epsilon^2)$ equations depend on the first-order solutions for x_1, y_1, z_1. Collecting only non-secular terms, we obtain

$$x_2'' - 2y_2' - \nu_{10}x_2 + \nu_{11}y_2 = \alpha_1\cos 2\tau_1 - \alpha_2\cos 2\tau_2 - \alpha_3 \sin 2\tau_1 + \alpha_4, \tag{71}$$

$$y_2'' + 2x_2' - \nu_{21}y_2 - \nu_{20}x_2 = -\delta_1 \sin 2\tau_1 + \delta_2\cos 2\tau_1 - \delta_3\cos 2\tau_2 + \delta_4, \tag{72}$$

$$z_2'' + \lambda^2 z_2 = -h_1[\sin(\tau_1 + \tau_2) + \sin(\tau_2 - \tau_1)] + h_2[\cos(\tau_2 - \tau_1) - \cos(\tau_1 + \tau_2)], \tag{73}$$

where all the coefficients are given in Appendix A.

We remove all the secular terms by setting $\omega_1 = 0$. Thus, we find the following solutions,

$$x_2 = \rho_{10} + \rho_{11}\cos 2\tau_1 + \rho_{12}\cos 2\tau_2 + \rho_{13}\sin 2\tau_2 + \rho_{14}\sin 2\tau_1, \tag{74}$$

$$y_2 = \rho_{20} + \rho_{21}\sin 2\tau_1 + \rho_{22}\sin 2\tau_2 - \rho_{23}\cos 2\tau_2 - \rho_{24}\cos 2\tau_1, \tag{75}$$

$$z_2 = \rho_{30}\sin(\tau_1 + \tau_2) + \rho_{31}\sin(\tau_2 - \tau_1) + \rho_{32}\cos(\tau_2 - \tau_1) + \rho_{33}\cos(\tau_1 + \tau_2), \tag{76}$$

where

$$\tau_1 = \lambda\tau + \phi, \qquad \text{and} \qquad \tau_2 = \lambda\tau + \psi. \tag{77}$$

All the coefficients are given in Appendix A.

3.5 Third-order equations

The $O(\epsilon^3)$ equations are obtained by setting $\omega_1 = 0$ and substituting in the solutions for x_1, y_1, z_1, x_2, y_2 and z_2. Thus, we obtain

$$x_3'' - 2y_3' - \nu_{10}x_3 + \nu_{11}y_3 = [\alpha_{11} + 2\omega_2\lambda^2 A_x(2\kappa - 1)]\cos\tau_1 + [\alpha_{12} + 2\kappa\lambda A_x\nu_{11}^2\omega_2]\sin\tau_1 + \alpha_{13}\cos 3\tau_1 + \alpha_{14}\cos(\tau_1 + 2\tau_2) + \alpha_{15}\cos(\tau_1 - 2\tau_2) + \alpha_{16}\sin(2\tau_2 + \tau_1) + \alpha_{17}\sin(2\tau_2 - \tau_1) + \alpha_{18}\sin 3\tau_1, \tag{78}$$

$$y_3'' + 2x_3' - \nu_{20}x_3 - \nu_{21}y_3 = [\alpha_{21} - 2\kappa\lambda^2 A_x\nu_{11}\omega_2]\cos\tau_1 + [\alpha_{22} + 2\lambda A_x\omega_2(2\kappa\lambda^2 - 1)]\sin\tau_1 + \alpha_{23}\cos 3\tau_1 + \alpha_{24}\cos(\tau_1 + 2\tau_2) + \alpha_{25}\cos(2\tau_2 - \tau_1) + \alpha_{26}\sin(2\tau_2 + \tau_1) + \alpha_{27}\sin(2\tau_2 - \tau_1) + \alpha_{28}\sin 3\tau_1, \tag{79}$$

$$z_3'' + \lambda^2 z_3 = \left[\alpha_{31} + A_z\left(2\omega_2\lambda^2 + \frac{\Delta}{\epsilon^2}\right)\right]\sin\tau_2 + \alpha_{32}\sin(2\tau_1 + \tau_2) + \alpha_{33}\sin(\tau_2 - 2\tau_1) + \alpha_{34}\sin 3\tau_2 + \alpha_{35}\cos\tau_2 + \alpha_{36}\cos 3\tau_2 + \alpha_{37}\cos(\tau_2 - 2\tau_1) + \alpha_{38}\cos(2\tau_1 + \tau_2), \tag{80}$$

where the expressions of the coefficients are given in Appendix A. There are secular terms. We start by examining the secular terms in the z_3 equation, by simply setting a value for the frequency correction ω_2. To remove the secular terms $\alpha_{33}\sin(\tau_2 - 2\tau_1)$ and $\alpha_{37}\cos(\tau_2 - 2\tau_1)$, we need the coefficients of these terms to be zero. Thus

$$\phi = \psi + n\frac{\pi}{2}, \qquad \text{where} \quad n = 0, 1, 2, 3.$$

The solution will be bounded if

$$\alpha_{31} + A_z\left(2\omega_2\lambda^2 + \frac{\Delta}{\epsilon^2}\right) - \zeta\alpha_{33} = 0, \tag{81}$$

and

$$\zeta\alpha_{37} = 0, \tag{82}$$

where $\zeta = (-1)^n$. This phase constraint affects the $x_3 - y_3$ equations; now each contains a secular term. The requirement of another constraint is from the simultaneous equations (78) and (79):

$$-(\nu_{11} + \lambda^2)[\alpha_{11} + 2\omega_2\lambda^2 A_x(2\kappa - 1)] + 2\lambda[\alpha_{22} + 2\lambda A_x\omega_2(2\kappa\lambda^2 - 1)] + \nu_{11}(\alpha_{21} - 2\kappa\lambda^2 A_x\nu_{11}\omega_2) + \zeta[-\alpha_{15}(\lambda^2 + \nu_{21}) + \lambda(\alpha_{27} + \nu_{11}\alpha_{25})] = 0, \tag{83}$$

and

$$-(\nu_{22} + \lambda^2)(\alpha_{12} + 2\kappa\lambda A_x\nu_{11}^2\omega_2) - 2\lambda(\alpha_{21} - 2\kappa\lambda^2 A_x\nu_{11}\omega_2) + \nu_{11}[\alpha_{22} + 2\lambda A_x\omega_2(2\kappa\lambda^2 - 1)] + \zeta[-\alpha_{17}(\lambda^2 + \nu_{21}) + \lambda(\alpha_{25} + \nu_{11}\alpha_{27})] = 0. \tag{84}$$

From these equations we find

$$\omega_2 = [\lambda^2\alpha_{11} + \zeta\lambda^2\alpha_{15} - 2\lambda\alpha_{22} - \zeta\lambda\alpha_{27} + \alpha_{11}\nu_{11} - \alpha_{21}\nu_{11} - \zeta(\lambda\alpha_{25}\nu_{11} - \alpha_{15}\nu_{21})]\{2\lambda^2 A_x[\lambda^2(2\kappa + 1) + \nu_{11} - 2\kappa\nu_{11} - \kappa\nu_{11}^2 - 2]\}^{-1}. \tag{85}$$

Table 3. At $\beta = 0.13$.

n	A_z	ω_2
0	±0.4202186	−24.7175
1	±0.1120075	−4.66144
2	±0.4202186	−24.7175
3	±0.1120075	−4.66144

Table 4. At $\beta = 0.15$.

n	A_z	ω_2
0	±0.219213958	−5.14832
1	±0.105566928	−3.32111
2	±0.219213958	−5.14832
3	±0.105566928	−3.32111

Table 5. At $\beta = 0.18$.

n	A_z	ω_2
0	±0.09654386	−0.718982
1	±0.05566177	−0.691666
2	±0.09654386	−0.718982
3	±0.05566177	−0.691666

The amplitude relation is obtained by putting the value of equation (85) into equation (81). Thus, we can satisfy this constraint by letting one amplitude be determined by the other.

Different amplitudes A_z at $A_x = 206\,000/(1.496 \times 10^8)$ with $sw = 0.35$ at different β and n are shown in Tables 3, 4 and 5. From these tables, we see that the amplitudes contract, whereas ω_2 decreases negatively when β increases. Using these constraints, the third-order equations are reduced to

$$x_3'' - 2y_3' - \nu_{10}x_3 + \nu_{11}y_3 = s_{11}\cos\tau_1 + s_{12}\sin\tau_1 + (\alpha_{13} + \zeta\alpha_{14})\cos 3\tau_1 + (\alpha_{18} + \zeta\alpha_{16})\sin 3\tau_1, \quad (86)$$

$$y_3'' + 2x_3' - \nu_{20}x_3 - \nu_{21}y_3 = s_{21}\cos\tau_1 + s_{22}\sin\tau_1 + (\alpha_{23} + \zeta\alpha_{24})\cos 3\tau_1 + (\alpha_{24} + \zeta\alpha_{26})\sin 3\tau_1, \quad (87)$$

$$z_3'' + \lambda^2 z_3 = \zeta(\alpha_{32}\sin 3\tau_1 + \alpha_{38}\cos 3\tau_1) + \alpha_{34}\begin{cases}(-1)^{n/2}\sin 3\tau_1, & n = 0, 2\\ (-1)^{(n-1)/2}\cos 3\tau_1, & n = 1, 3\end{cases} + \alpha_{36}\begin{cases}(-1)^{n/2}\cos 3\tau_1, & n = 0, 2\\ (-1)^{(n+1)/2}\sin 3\tau_1, & n = 1, 3.\end{cases} \quad (88)$$

The solutions are

$$x_3 = \sigma_{10}\cos\tau_1 + \sigma_{11}\sin\tau_1 + \sigma_{12}\cos 3\tau_1 + \sigma_{13}\sin 3\tau_1, \quad (89)$$

$$y_3 = \sigma_{20}\cos\tau_1 + \sigma_{21}\sin\tau_1 + \sigma_{22}\cos 3\tau_1 + \sigma_{23}\sin 3\tau_1, \quad (90)$$

$$z_3 = \frac{1}{8\lambda^2}\left[\zeta(\alpha_{32}\sin 3\tau_1 + \alpha_{38}\cos 3\tau_1) + \begin{cases}(-1)^{n/2}(\alpha_{34}\sin 3\tau_1 + \alpha_{36}\cos 3\tau_1), n = 0, 2\\ (-1)^{(n-1)/2}(\alpha_{34}\cos 3\tau_1 - \alpha_{36}\sin 3\tau_1), n = 1, 3\end{cases}\right], \quad (91)$$

where the expressions of the coefficients are given in Appendix A.

3.6 Final approximation

Using all the first-, second- and third-order approximate solutions with the mapping $A_x \mapsto A_x/\epsilon$ and $A_z \mapsto A_z/\epsilon$, which remove ϵ from all the equations, we obtain

$$x(\tau) = \rho_{10} + (-A_x + \sigma_{10})\cos\tau_1 + \sigma_{11}\sin\tau_1 + (\rho_{11} + \zeta\rho_{12})\cos 2\tau_1 + (\rho_{14} + \zeta\rho_{13})\sin 2\tau_1 + \sigma_{12}\cos 3\tau_1 + \sigma_{13}\sin 3\tau_1, \quad (92)$$

$$y(\tau) = \rho_{20} + (2\lambda\kappa A_x + \sigma_{21})\sin\tau_1 + (-\kappa A_x \nu_{11} + \sigma_{20})\cos\tau_1 + (\rho_{21} + \zeta\rho_{22})\sin 2\tau_1 - (\rho_{24} + \zeta\rho_{23})\cos 2\tau_1 + \sigma_{22}\cos 3\tau_1 + \sigma_{23}\sin 3\tau_1 \quad (93)$$

and

$$z(\tau) = A_z\begin{cases}(-1)^{(n+4)/2}(A_z\sin\tau_1 + \rho_{30}\sin 2\tau_1), n = 0, 2\\ (-1)^{(n+1)/2}(A_z\cos\tau_1 + \rho_{30}\cos 2\tau_1), n = 1, 3\end{cases} + \rho_{31}\begin{cases}0, n = 0, 2\\ (-1)^{(n+1)/2}, n = 1, 3\end{cases} + \rho_{32}\begin{cases}(-1)^{n/2}, n = 0, 2\\ 0, n = 1, 3\end{cases} - \frac{1}{8\lambda^2}\left[\zeta(\alpha_{32}\sin 3\tau_1 + \alpha_{38}\cos 3\tau_1) + \begin{cases}(-1)^{n/2}(\alpha_{34}\sin 3\tau_1 + \alpha_{36}\cos 3\tau_1), n = 0, 2\\ (-1)^{(n-1)/2}(\alpha_{34}\cos 3\tau_1 - \alpha_{36}\sin 3\tau_1), n = 1, 3\end{cases}\right]. \quad (94)$$

The expressions of the coefficients are given in Appendix A.

For the Sun–(Earth–Moon) L_1, the difference of both frequencies of the z-plane and xy-plane is quite small. The values of A_x and A_z are found using the relation of equations (85) and (81).

In the final approximation, the halo orbits at $n = 0$ and 2 with $sw = 0.35$ are shown in Figs 10, 12 and 14. For $n = 1$ and 3, the halo orbits are depicted in Figs 11, 13 and 15. The amplitude and frequency ω_2 are both equal for each case, $n = 0$, 2 and $n = 1$, 3. When β increases, then the trajectory shrinks.

In the previous subsections, we have computed the first, second, third and final approximations for the halo orbits and we have seen the effect of radiation pressure, with P–R drag and solar wind drag. In the absence of drag forces, the results agree with those of the classical case (Thurman & Worfolk 1996)

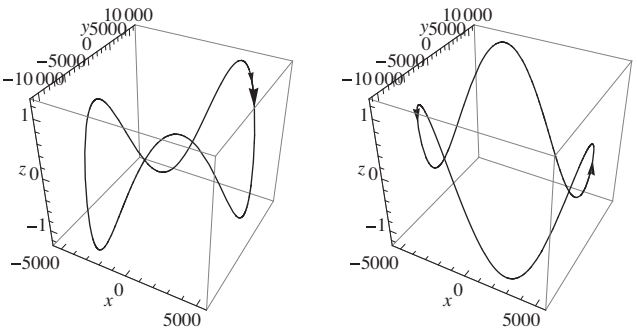

Figure 10. Halo orbit at $n = 0$ and $n = 2$ at $\beta = 0.13$.

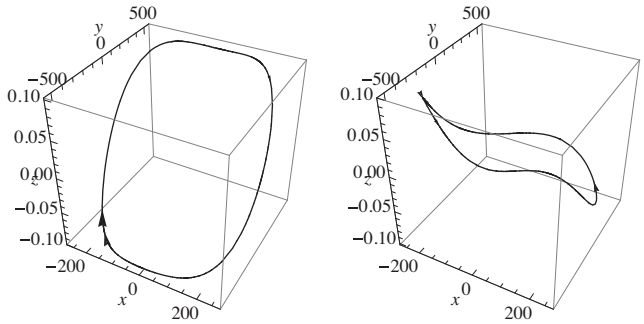

Figure 11. Halo orbit at $n = 1$ and $n = 3$ at $\beta = 0.13$.

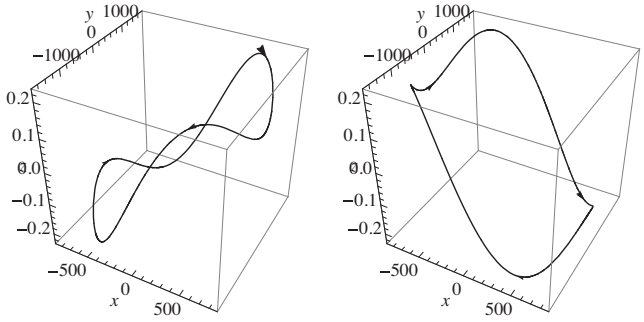

Figure 12. Halo orbit at $n = 0$ and $n = 2$ at $\beta = 0.15$.

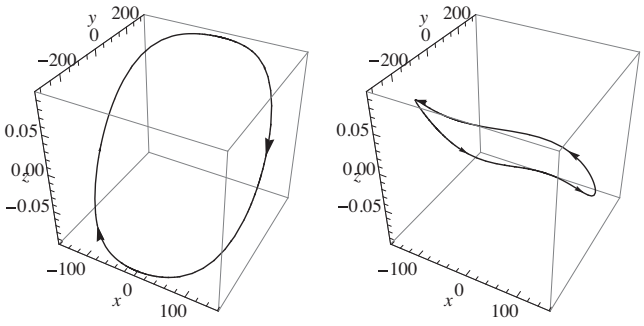

Figure 13. Halo orbit at $n = 1$ and $n = 3$ at $\beta = 0.15$.

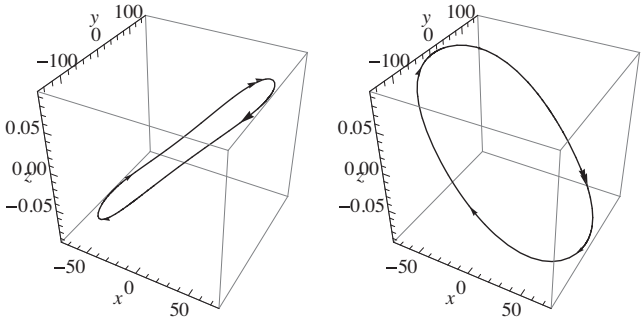

Figure 14. Halo orbit at $n = 0$ and $n = 2$ at $\beta = 0.18$.

4 CONCLUSIONS

In this paper, we have studied the circular restricted three-body problem of the Sun–Earth–Moon system by assuming the effect of radiation pressure, P–R drag and solar wind drag. We have found that the collinear Lagrangian points deviate from their axis joining the primaries, whereas the triangular points remain unchanged in their configuration. However, all points lie in a plane. If we increase the value of β, with a fixed value of $sw = 0.35$, the Lagrangian points L_1, L_2 and L_3 tend towards the radiating body (the Sun), whereas $L_{4,5}$ have symmetrical changes with the increasing value of β. We have examined the linear stability of the equilibrium points with the help of characteristic roots. It is observed that the Lagrangian points are unstable because of the drag forces. Furthermore, we have computed the orbit around the L_1 point and have seen that when radiation pressure increases, the phase difference of the trajectory decreases. If there is no drag force (i.e. $\beta = 0$), then the trajectory of the Lissajous orbit completes one period approximately at $t = 3.0$, whereas if β increases with $sw = 0.35$, it does not complete its period at the same time. Also, because of the increasing value of β, the trajectories shrink in its amplitude. In this study, we have used the Lindstedt–Poincaré method to compute the halo orbits in the third-order approximation with the radiation pressure, P–R drag and solar wind drag. In this analysis, we have fixed the value of $sw = 0.35$, which is the ratio of solar wind drag to P–R drag, and we have varied the value of β (i.e. the ratio of radiation pressure force to solar gravitation force). This model can be used to compute the higher-order approximation (four, fifth, etc.) expressions for halo orbits. Moreover, stable and unstable manifolds of the halo orbits, and trajectory transfer, would be interesting topics of future research with similar dissipative forces.

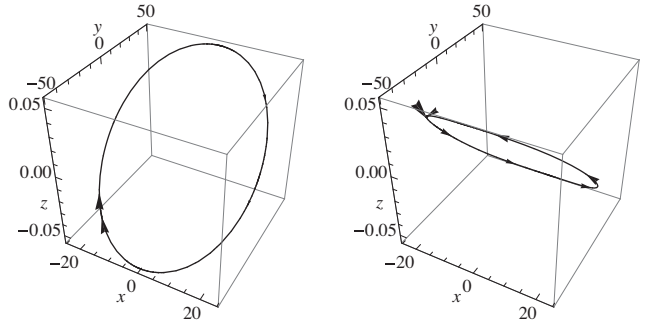

Figure 15. Halo orbit at $n = 1$ and $n = 3$ at $\beta = 0.18$.

ACKNOWLEDGEMENTS

We are grateful to Inter-University Centre for Astronomy and Astrophysics (IUCAA), Pune for supporting library visits and for the use of computing facilities. BSK is also grateful to the Indian Space Research Organization (ISRO), Department of Space, Government of India, for providing financial support through the RESPOND Programme (Project No -ISRO/RES/2/383/2012-13).

REFERENCES

Breakwell J., Brown J., 1979, Celestial Mechanics, 20, 389
Burns J. A., Lamy P. L., Soter S., 1979, Icarus, 40, 1
Calleja R. C., Doedel E. J., Humphries A. R., Lemus-Rodríguez A., Oldeman E. B., 2012, Celestial Mechanics and Dynamical Astronomy, 114, 77
Clarke T. L., 2003, Bull. Am. Astron. Soc., 35, 1204
Clarke T., 2005, APS April Meeting, Abstract C9007
Di Giamberardino P., Monaco S., 1992, in Proc. 31st IEEE Conf. on Decision and Control. IEEE, New York, p. 536
Eapen R. T., Sharma R. K., 2014, Ap&SS, 352, 437
Farquhar R. W., 2001, Journal of the Astronautical Sciences, 49, 23
Farquhar R. W., Muhonen D. P., Richardson D. L., 1977, Journal of Spacecraft and Rockets, 14, 170

Folta D., Pavlak T., Haapala A., Howell K., 2013, in 23rd AAS/AIAA Space Flight Mechanics Meeting
Gustafson B. A. S., 1994, Annual Review of Earth and Planetary Sciences, 22, 553
Hill K. A., Born G. H., 2008, Journal of Spacecraft and Rockets, 45, 548
Howell K. C., 1984, Celestial Mechanics, 32, 53
Ishwar B., Kushvah B., 2006, Journal of Dynamical Systems and Geometric Theories, 4, 79
Junge O., Levenhagen J., Seifried A., Dellnitz M., 2002, Earth, 1, L3
Kim M., Hall C. D., 2001, in Proc. AAS/AIAA Astrodynamics Specialist Conference, Vol. 109. American Astronautical Society, Springfield, VA, p. 349
Kolemen E., Kasdin N. J., Gurfil P., 2007, in Belbruno E., ed, AIP Conf. Proc. Vol. 886, New Trends in Astrodynamics and Applications III. American Institute of Physics, New York, p. 68
Kumari R., Kushvah B. S., 2013, Ap&SS, 344, 347
Kushvah B. S., 2008, Ap&SS, 315, 231
Liou J-C., Zook H. A., Jackson A. A., 1995, Icarus, 116, 186
Murray C. D., 1994, Icarus, 112, 465
Murray C., Dermott S., 1999, Solar System Dynamics. Cambridge Univ. Press, Cambridge
Parker E. N., 1965, Space Sci. Rev., 4, 666
Pavlak T., Howell K., 2012, in AIAA/AAS Astrodynamics Specialist Conference
Richardson D. L., 1980, Celestial Mechanics, 22, 241
Schuerman D. W., 1980, ApJ, 238, 337
Simmons J. F. L., McDonald A. J. C., Brown J. C., 1985, Celestial Mechanics, 35, 145
Thurman R., Worfolk P. A., 1996, Technical report, The Geometry of Halo Orbits in the Circular Restricted Three-Body Problem

APPENDIX A: COEFFICIENTS

$$a_{00} = (a^* - d^* - 1)(a^* - b^* - 1) - c^{*2}, \tag{A1}$$

$$a_{20} = 2(1 + a^*) - b^* - d^*, \tag{A2}$$

$$a_3 = -(1 + sw)(K_{x,\dot{x}} + K_{y,\dot{y}}), \tag{A3}$$

$$a_2 = -(1 + sw)[K_{x,x} + K_{y,y} - 2(K_{x,\dot{y}} - K_{y,\dot{x}})], \tag{A4}$$

$$a_1 = (1 + sw)[(1 - a^* + b^*)K_{x,\dot{x}} + (1 - a^* + d^*)K_{y,\dot{y}} + 2(K_{x,y} - K_{y,x}) - c^*(K_{x,\dot{y}} + K_{y,\dot{x}})], \tag{A5}$$

$$a_0 = (1 + sw)[(1 - a^* + b^*)K_{x,x} + (1 - a^* + d^*)K_{y,y} - c^*(K_{x,y} + K_{y,y})], \tag{A6}$$

$$\zeta_1 = \nu_{20}\nu_{11} + \nu_{10}\nu_{21}, \tag{A7}$$

$$\nu_{10} = 1 - (c_2 + d_2) + 3\left[\frac{c_2(\gamma - 1)^2}{D_1^2} + \frac{d_2\gamma^2}{D_2^2}\right] + \frac{(1 + sw)\beta(1 - \mu)}{c} \times \left[\frac{\mu l + 2l(\gamma - 1)}{D_1^4} - \frac{4\mu(\gamma - 1)^2 l}{D_1^6}\right], \tag{A8}$$

$$\nu_{11} = 3l\left[\frac{c_2(\gamma - 1)}{D_1^2} + \frac{d_2\gamma}{D_2^2}\right] + \frac{(1 + sw)\beta(1 - \mu)}{c}\left[\frac{\mu(\gamma - 1)}{D_1^4} - \frac{1}{D_1^2}\right], \tag{A9}$$

$$\nu_{12} = \frac{15}{2}\left[\frac{c_3(\gamma - 1)^3}{D_1^3} + \frac{d_3\gamma^3}{D_2^3}\right] - \frac{9}{2} \times \left[\frac{c_3(\gamma - 1)}{D_1} + \frac{d_3\gamma}{D_2}\right] + \frac{(1 + sw)\beta(1 - \mu)}{c} \times \left[\frac{6\mu(\gamma - 1)l + 4l(\gamma - 1)}{D_1^6} - \frac{l}{D_1^4} - \frac{12\mu l(\gamma - 1)^3}{D_1^8}\right], \tag{A10}$$

$$\nu_{13} = -\frac{3}{2}\left[\frac{c_3(\gamma - 1)}{D_1} + \frac{d_3\gamma}{D_2}\right] + \frac{(1 + sw)\beta(1 - \mu)}{c} \times \left[\frac{4\mu(\gamma - 1)l}{D_1^6} - \frac{2l}{D_1^4}\right], \tag{A11}$$

$$\nu_{14} = \frac{-3}{2}\left[\frac{c_3(\gamma - 1)}{D_1} + \frac{d_3\gamma}{D_2}\right] + \frac{(1 + sw)\beta(1 - \mu)}{c}\left[\frac{2\mu l(\gamma - 1)}{D_1^6} - \frac{l}{D_1^4}\right], \tag{A12}$$

$$\nu_{17} = \frac{15l}{2}\left[\frac{c_4(\gamma - 1)}{D_1^2} + \frac{d_4\gamma}{D_2^2}\right] \times \frac{(1 + sw)\beta(1 - \mu)}{c}\left[\frac{2\mu(\gamma - 1)}{D_1^6} - \frac{1}{D_1^4}\right], \tag{A13}$$

$$\nu_{15} = 15l\left[\frac{c_3(\gamma - 1)^2}{D_1^3} + \frac{d_3\gamma^2}{D_2^3}\right] - 3l\left(\frac{c_3}{D_1} + \frac{d_3}{D_2}\right) + \frac{105l}{2}\left[\frac{c_4(\gamma - 1)^3}{D_1^4} + \frac{d_4\gamma^3}{D_2^4}\right] - \frac{(1 + sw)\beta(1 - \mu)}{c}\left[\frac{\mu + 2(\gamma - 1)}{D_1^4} - \frac{4\mu(\gamma - 1)^2}{D_1^6}\right], \tag{A14}$$

$$\nu_{16} = -15\left[\frac{c_4(\gamma - 1)^2}{D_1^2} + \frac{d_4\gamma^2}{D_2^2}\right] + \frac{35}{2}\left[\frac{c_4(\gamma - 1)^4}{D_1^4} + \frac{d_4(\gamma - 1)^2}{D_2^4}\right] + \frac{3}{2}(c_4 + d_4) + \frac{(1 + sw)\beta(1 - \mu)}{c}\left\{\frac{24l\mu(\gamma - 1)^2 + 8l(\gamma - 1)^3}{D_1^8} - \frac{28[(\gamma - 1)^4 l\mu]}{D_1^{10}} - \frac{2\mu l + 4(\gamma - 1)l}{D_1^6}\right\}, \tag{A15}$$

$$\nu_{18} = -\frac{15}{2}\left[\frac{c_4(\gamma - 1)^2}{D_1^2} + \frac{d_4\gamma^2}{D_2^2}\right] + \frac{3}{2}(c_4 + d_4) + \frac{(1 + sw)\beta(1 - \mu)}{c}\left[\frac{-6\mu l - 12l(\gamma - 1)}{D_1^6} + \frac{(24\mu l - 12\mu)(\gamma - 1)^2}{D_1^8}\right], \tag{A16}$$

$$\nu_{19} = \frac{-15}{2}\left[\frac{c_4(\gamma-1)^2}{D_1^2} + \frac{d_4\gamma^2}{D_2^2}\right] + \frac{3}{2}(c_4+d_4) + \frac{(1+sw)\beta(1-\mu)}{c}\left[-\frac{2\mu l + 4(\gamma-1)l}{D_1^6} - \frac{12\mu(\gamma-1)^2 l}{D_1^8}\right], \quad \text{(A17)}$$

$$\nu^* = 1-\mu-\gamma+\frac{c_1(\gamma-1)}{D_1} + \frac{d_1\gamma}{D_2} + \frac{(1+sw)\beta(1-\mu)}{c}\left[\frac{l}{D_1^2} - \frac{\mu l(\gamma-1)}{D_1^4}\right], \quad \text{(A18)}$$

$$\nu_{20} = -3l\left[\frac{c_2(\gamma-1)}{D_1^2} + \frac{d_2\gamma}{D_2^2}\right] - \frac{(1+sw)\beta(1-\mu)}{c} \times \left[\frac{2(\gamma-1)(1-\mu-\gamma)}{D_1^4} + \frac{1}{D_1^2}\right], \quad \text{(A19)}$$

$$\nu_{21} = 1-c_2-d_2-\frac{2(1+sw)\beta(1-\mu)(\gamma-1)l}{cD_1^4}, \quad \text{(A20)}$$

$$\nu_{22} = -\frac{15}{2}l\left[\frac{c_3(\gamma-1)^2}{D_1^3} + \frac{d_3\gamma^2}{D_2^3}\right] + \frac{3l}{2}\left(\frac{c_3}{D_1} + \frac{d_3}{D_2}\right) + \frac{(1+sw)\beta(1-\mu)}{c} \times \left[\frac{3(1-\gamma)-\mu}{D_1^4} - \frac{4(\gamma-1)^2(1-\mu-\gamma)}{D_1^6}\right], \quad \text{(A21)}$$

$$\nu_{23} = \frac{9l}{2}\left(\frac{c_3}{D_1} + \frac{d_3}{D_2}\right) - \frac{(1+sw)\beta(1-\mu)}{c}\left[\frac{(\gamma-1)}{D_1^4}\right], \quad \text{(A22)}$$

$$\nu_{24} = \frac{3l}{2}\left(\frac{c_3}{D_1} + \frac{d_3}{D_2}\right) + \frac{(1+sw)\beta(1-\mu)(1-\mu-\gamma)}{cD_1^4}, \quad \text{(A23)}$$

$$\nu_{25} = -3\left[\frac{c_3(\gamma-1)}{D_1} + \frac{d_3\gamma}{D_2}\right] + \frac{(1+sw)\beta(1-\mu)}{c} \times \left\{\frac{8l(\gamma-1)^2 l[-3(\mu+\gamma)+2]}{D_1^6} + \frac{2l}{D_1^4}\right\}, \quad \text{(A24)}$$

$$\nu_{30} = -3\left[\frac{c_3(\gamma-1)}{D_1} + \frac{d_3\gamma}{D_2}\right] + \frac{4(1+sw)\beta\mu(1-\mu)(\gamma-1)l}{cD_1^6}, \quad \text{(A25)}$$

$$\nu_{31} = 3l\left(\frac{c_3}{D_1} + \frac{d_3}{D_2}\right) + \frac{(1+sw)\beta\mu(1-\mu)}{cD_1^4}, \quad \text{(A26)}$$

$$\nu_{190} = \frac{45l}{2}\left[\frac{c_4(\gamma-1)}{D_1^2} + \frac{d_4\gamma}{D_2^2}\right] + \frac{(1+sw)\beta}{c} \times \left[\frac{6\mu(\gamma-1)+4(\gamma-1)^2}{D_1^6} - \frac{1}{D_1^4} - \frac{12\mu(\gamma-1)^3}{D_1^8}\right], \quad \text{(A27)}$$

$$\nu_{191} = \frac{15l}{2}\left[\frac{c_4(\gamma-1)}{D_1^2} + \frac{d_4\gamma}{D_2^2}\right] + \frac{(1+sw)\beta(1-\mu)}{c}\left[\frac{2\mu(\gamma-1)}{D_1^6} - \frac{1}{D_1^4}\right], \quad \text{(A28)}$$

$$\nu^* = 1-mu-\gamma+\frac{c_1(\gamma-1)}{D_1} + \frac{d_1\gamma}{D_2} + \frac{(1+sw)\beta(1-\mu)}{c}\left[\frac{\mu l(1-\gamma)}{D_1^4} + \frac{l}{D_1^2}\right], \quad \text{(A29)}$$

$$\nu_{26} = -\frac{35l}{2}\left[\frac{c_4(\gamma-1)^3}{D_1^4} + \frac{d_4\gamma^3}{D_2^4}\right] + \frac{15l}{2}\left[\frac{c_4(\gamma-1)}{D_1^2} + \frac{d_4\gamma}{D_2^2}\right] + \frac{(1+sw)\beta(1-\mu)}{c} \times \left[\frac{1}{D_1^4} - \frac{8(\gamma-1)^2+4\mu(\gamma-1)}{D_1^6} - \frac{8(\gamma-1)^3(1-\mu-\gamma)}{D_1^8}\right], \quad \text{(A30)}$$

$$\nu_{27} = \frac{3}{2}(c_4+d_4) + \frac{(1+sw)\beta(1-\mu)}{c}\frac{4l(\gamma-1-\mu)}{D_1^6}, \quad \text{(A31)}$$

$$\nu_* = c_2+d_2-\frac{(1+sw)\beta(1-\mu)\mu l}{cD_1^4}, \quad \text{(A32)}$$

$$\nu_{29} = \frac{45l}{2}\left[\frac{c_4(\gamma-1)}{D_1^2} + \frac{d_4\gamma}{D_2^2}\right] + \frac{(1+sw)\beta(1-\mu)}{c}\left[\frac{1}{D_1^4} - \frac{4(\gamma-1)^2}{D_1^6}\right], \quad \text{(A33)}$$

$$\nu_{290} = \frac{15l}{2}\left[\frac{c_4(\gamma-1)}{D_1^2} + \frac{d_4\gamma}{D_2^2}\right] + \frac{(1+sw)\beta(1-\mu)}{c} \times \left[\frac{1}{D_1^4} + \frac{4(\gamma-1)(1-\mu-\gamma)}{D_1^6}\right], \quad \text{(A34)}$$

$$\nu_{291} = -\frac{15}{2}\left[\frac{c_4(\gamma-1)^2}{D_1^2} + \frac{d_4\gamma^2}{D_2^2}\right] + \frac{3}{2}(c_4+d_4) + \frac{(1+sw)\beta(1-\mu)}{c} \times \left[\frac{12l(\gamma-1)}{D_1^6} - \frac{24l(\gamma-1)^2(\mu+1)}{D_1^8}\right], \quad \text{(A35)}$$

$$\nu_{292} = \frac{3}{2}(c_4+d_4) + \frac{(1+sw)\beta(1-\mu)}{c}\left[\frac{4l(\gamma-1)}{D_1^6}\right], \quad \text{(A36)}$$

$$\nu^{**} = l\left[1-\left(\frac{c_1}{D_1} + \frac{d_1}{D_2}\right)\right] + \frac{(1+sw)\beta(1-\mu)}{c}\frac{(\gamma-1+\mu)}{D_1^2}, \quad \text{(A37)}$$

$$\nu_{32} = \frac{-15}{2}\left[\frac{c_4(\gamma-1)^2}{D_1^2} + \frac{d_4\gamma^2}{D_2^2}\right] + \frac{3}{2}(c_4+d_4) + \frac{(1+sw)\beta(1-\mu)\mu l}{cD_1^4}\left[\frac{12(\gamma-1)^2}{D_1^4} - \frac{2}{D_1^2}\right], \quad \text{(A38)}$$

$$\nu_{33} = 15l\left[\frac{c_4(\gamma-1)}{D_1^2} + \frac{d_4\gamma}{D_2^2}\right] + \frac{4(1+sw)\beta(1-\mu)\mu(\gamma-1)}{cD_1^6}, \quad \text{(A39)}$$

$$\nu_{34} = \frac{3}{2}(c_4+d_4) - \frac{6(1+sw)\beta(1-\mu)\mu l}{cD_1^6}, \quad \text{(A40)}$$

$$\nu_{35} = \frac{3}{2}(c_4+d_4) - \frac{2(1+sw)\beta(1-\mu)\mu l}{cD_1^6}, \quad \text{(A41)}$$

$$\rho_{10} = -\frac{A_{14}}{\nu_{10}\nu_{21} - \nu_{20}\nu_{11}}, \quad \text{(A42)}$$

$$\rho_{11} = \frac{-A_{11}B_{11} + 4\lambda A_{13}(\nu_{11}-\nu_{20})}{B_{11}^2 + 16\lambda^2(\nu_{11}-\nu_{20})^2}, \quad \text{(A43)}$$

$$\rho_{12} = \frac{B_{11}A_{12}}{B_{11}^2 + 16\lambda^2(\nu_{11}-\nu_{20})^2}, \quad \text{(A44)}$$

$$\rho_{13} = \frac{B_{11}A_{13} - 4A_{12}\lambda(\nu_{11}-\nu_{20})}{B_{11}^2 + 16\lambda^2(\nu_{11}-\nu_{20})^2}, \quad \text{(A45)}$$

$$\rho_{14} = \frac{4A_{11}\lambda(\nu_{11}-\nu_{20})}{B_{11}^2 + 16\lambda^2(\nu_{11}-\nu_{20})^2}, \quad \text{(A46)}$$

$$\rho_{20} = \frac{-\delta_4 + \nu_{31}\rho_{10}}{\nu_{21}}, \quad \text{(A47)}$$

$$\rho_{21} = \frac{4\lambda\rho_{11} - \nu_{31}\rho_{14} - \delta_1}{-4\lambda^2 - \nu_{21}}, \quad \text{(A48)}$$

$$\rho_{22} = \frac{4\lambda\rho_{12} - \nu_{31}\rho_{13}}{-4\lambda^2 - \nu_{21}}, \quad \text{(A49)}$$

$$\rho_{23} = \frac{4\lambda\rho_{13} + \nu_{31}\rho_{12} + \delta_3}{-4\lambda^2 - \nu_{21}}, \quad \text{(A50)}$$

$$\rho_{24} = \frac{4\lambda + \nu_{31}\rho_{11} - \delta_2}{-4\lambda^2 - \nu_{21}}, \quad \text{(A51)}$$

$$\rho_{30} = \frac{h_1}{-3\lambda^2}, \quad \text{(A52)}$$

$$\rho_{31} = \frac{h_1}{\lambda^2}, \quad \text{(A53)}$$

$$\rho_{32} = \frac{h_2}{\lambda^2}, \quad \text{(A54)}$$

$$\rho_{33} = \frac{h_2}{-3\lambda^2}, \quad \text{(A55)}$$

$$A_{11} = 4\lambda^2\alpha_1 + \alpha 1\nu_{21} + 4\lambda\delta_1 + \delta_2\nu_{11}, \quad \text{(A56)}$$

$$A_{12} = 4\lambda^2\alpha_2 + \alpha_2\nu_{21} + \delta_3\nu_{11}, \quad \text{(A57)}$$

$$A_{13} = 4\lambda^2\alpha_3 + \nu_{21}\alpha_3 - 4\delta_2\lambda + \delta_1\nu_{11}, \quad \text{(A58)}$$

$$A_{14} = \alpha_2\nu_{21} + \nu_{11}\delta_4, \quad \text{(A59)}$$

$$B_{11} = 16\lambda^4 - 4\lambda^2(4 - \nu_{21} + \nu_{10}) + (\nu_{10}\nu_{21} - \nu_{20}\nu_{11}), \quad \text{(A60)}$$

$$s_{11} = \alpha_{11} + 2\omega_2\lambda^2 A_x(2\kappa - 1), \quad \text{(A61)}$$

$$s_{12} = \alpha_{12} + 2\kappa\lambda A_x\nu_{11}^2\omega_2, \quad \text{(A62)}$$

$$\sigma_{10} = \frac{\beta_{11}\beta_{21} + \beta_{12}\beta_{22}}{\beta_{21}^2 + \beta_{22}^2}, \quad \text{(A63)}$$

$$\sigma_{11} = \frac{\beta_{12}\beta_{21} - \beta_{11}\beta_{22}}{\beta_{21}^2 + \beta_{22}^2}, \quad \text{(A64)}$$

$$\sigma_{12} = \frac{\beta_{13}\beta_{31} + \beta_{14}\beta_{32}}{\beta_{31}^2 + \beta_{32}^2}, \quad \text{(A65)}$$

$$\sigma_{13} = \frac{\beta_{14}\beta_{31} - \beta_{13}\beta_{31}\beta_{32}}{\beta_{31}^2 + \beta_{22}^2}, \quad \text{(A66)}$$

$$c_n = \frac{(1-\beta)(1-\mu)}{D_1^{n+1}}, \qquad d_n = \frac{\mu}{D_2^{n+1}}, \quad \text{(A67)}$$

$$D_1 = \sqrt{(\gamma-1)^2 + l^2}, \quad \text{(A68)}$$

$$D_2 = \sqrt{\gamma^2 + l^2}, \quad \text{(A69)}$$

$$\beta_{11} = -s_{11}\lambda^2 + \nu_{21}s_{11} + 2s_{22}\lambda - \nu_{11}s_{21}, \quad \text{(A70)}$$

$$\beta_{12} = -s_{12}\lambda^2 - \nu_{21}s_{12} - 2s_{21}\lambda - \nu_{11}s_{22}, \quad \text{(A71)}$$

$$\beta_{13} = -9\lambda^2(\alpha_{13} + \zeta\alpha_{14}) - \nu_{21}(\alpha_{13} + \zeta\alpha_{14}) + 3\lambda(\alpha_{24} + \zeta\alpha_{26}) - \nu_{11}(\alpha_{23} + \zeta\alpha_{24}), \quad \text{(A72)}$$

$$\beta_{14} = -9\lambda^2(\alpha_{18} + \zeta\alpha_{16}) - \nu_{21}(\alpha_{18} + \zeta\alpha_{16}) - 3\lambda(\alpha_{23} + \zeta\alpha_{24}) - \nu_{11}(\alpha_{24} + \zeta\alpha_{26}), \quad \text{(A73)}$$

$$\beta_{21} = \lambda^4 - \lambda^2(4 - \nu_{21} - \nu_{10}) + \nu_{10}\nu_{21} + \nu_{11}\nu_{20}, \quad \text{(A74)}$$

$$\beta_{22} = 2\lambda(\nu_{11} + \nu_{20}), \quad \text{(A75)}$$

$$\beta_{31} = 81\lambda^4 - 9\lambda^2(4 - \nu_{21} - \nu_{10}) + \nu_{10}\nu_{21} + \nu_{11}\nu_{20}, \quad \text{(A76)}$$

$$\beta_{32} = 6\lambda(\nu_{11} + \nu_{20}), \quad \text{(A77)}$$

$$\sigma_{20} = \frac{-2\sigma_{11}\lambda + \nu_{20}\sigma_{10} + s_{21}}{-\lambda^2 - \nu_{21}}, \tag{A78}$$

$$\sigma_{21} = \frac{2\sigma_{10}\lambda + \nu_{20}\sigma_{11} + s_{22}}{-\lambda^2 - \nu_{21}}, \tag{A79}$$

$$\sigma_{22} = \frac{-6\sigma_{13}\lambda + \nu_{20}\sigma_{12} + \alpha_{23} + \zeta\alpha_{24}}{-9\lambda^2 - \nu_{21}}, \tag{A80}$$

$$\alpha_1 = \frac{\nu_{21}A_x^2 + \nu_{13}\kappa^2 A_x^2 \nu_{10}^2}{2} - 2\nu_{13}\kappa^2 A_x^2\lambda^2, \tag{A81}$$

$$\alpha_2 = \frac{\nu_{14}A_z^2}{2}, \qquad \alpha_3 = 2\nu_{13}\kappa^2 A_x^2\lambda\nu_{10}, \tag{A82}$$

$$\alpha_4 = \frac{\nu_{12}A_x^2 + \nu_{13}\kappa^2 A_x^2 \nu_{10}^2}{2} + \frac{\nu_{14}A_z^2}{2} + 2\nu_{13}\kappa^2 A_x^2\lambda^2, \tag{A83}$$

$$\delta_1 = \nu_{25}\kappa A_x^2\lambda - 2\lambda\nu_{10}\nu_{23}\kappa^2 A_x^2, \tag{A84}$$

$$\delta_2 = \frac{\nu_{22}A_x^2 - (\nu_{25} + \nu_{23}\kappa)\kappa A_x^2\nu_{10}}{2} - 2\lambda^2\nu_{23}\kappa^2 A_x^2, \tag{A85}$$

$$\delta_3 = \frac{\nu_{24}A_z^2}{2}, \tag{A86}$$

$$\delta_4 = \frac{(\nu_{22} - \nu_{25}\kappa\nu_{10} + \nu_{23}\kappa^2\nu_{10}^2 + 2\lambda_2\kappa^2\nu_{23})A_x^2 + \nu_{24}A_z^2}{2}, \tag{A87}$$

$$h_1 = \frac{(\nu_{30} + \nu_{31})A_x A_z}{2}, \tag{A88}$$

$$h_2 = \lambda\nu_{31}\kappa A_x A_z. \tag{A89}$$

This paper has been typeset from a TEX/LATEX file prepared by the author.